Kwon et al. Int J Concr Struct Mater (2025) 19:20
https://doi.org/10.1186/s40069-024-00758-w

International Journal of Concrete Structures and Materials

RESEARCH Open Access

# Probabilistic Analysis of Chloride Ingress Repair Costs Considering External Forces and Vulnerable Sections of RC Girders

Seung-Jun Kwon[1], Kwang-Mo Lim[2], Kyong-Chul Kim[2], Kyung-Taek Koh[2] and Yong-Sik Yoon[2*]

**Abstract**

This study analyzed the chloride ingress repair costs for RC girders by considering cold joints and external force conditions. The diffusion behavior of chloride ions, which varies with the stress conditions, was quantified. A two-span RC continuous girder was assumed to evaluate the magnitude of stress in each section under cracking load, and these results were comprehensively considered along with the quantification of chloride ion diffusion behavior. Then, the change in chloride ion diffusion behavior owing to external forces on the RC girders was analyzed to evaluate the service life under chloride ingress. At the locations with cold joints, the service life decreased by up to 33.9% owing to the higher baseline diffusion coefficient in the cold joint areas than that in sound concrete and significant increase in the diffusion coefficient with increased stress. Furthermore, this study analyzed the chloride ingress repair costs required to achieve the target service life of the RC structure with consideration of the external forces and cold joints using deterministic and probabilistic analyses methods. Probabilistic analysis offers the advantage of deriving the repair frequency and cost results in the form of continuous functions. Considering the four main points of the structure under analysis, the maintenance costs were evaluated at 2777.6 $/m$^2$ in the deterministic analysis and 2337.6$/m$^2$ in the probabilistic analysis. A repair cost analysis flowchart that integrates various repair processes can facilitate the analysis of repair processes that have a dominant influence on the overall maintenance cost estimation of RC girders.

**Keywords** Chloride ingress, Stress conditions, Cold joint, Repair cost, Probabilistic analysis

## 1 Introduction

Concrete is a construction material with high durability and mechanical performance, but as a porous medium, it allows the penetration of various degradation factors such as moisture. Among the typical degradation phenomena caused by the diffusion of various degradation factors into concrete are freeze–thaw damage due to moisture penetration in winter; carbonation from the reaction of carbon dioxide with moisture in the pores, reducing the pH of the pore water; and chloride ingress caused by diffused chloride ions (Mehta & Monteiro, 2009). In particular, carbonation and chloride ingress cause corrosion of the internal reinforcement of the concrete. Initially, corrosion affects only the esthetics of the structural surface owing to the formation of cracks and rust stains, but ultimately leads to problems with the load-bearing capacity of the reinforcement, necessitating special attention (Koh et al., 2019; Lee & Zielske, 2014; Yoon et al., 2018).

Journal information: ISSN 1976-0485 / eISSN 2234-1315.

*Correspondence:
Yong-Sik Yoon
humbleyys@kict.re.kr
[1] Department of Civil and Environmental Engineering, Hannam University, Daejeon 34430, Republic of Korea
[2] Korea Institute of Civil Engineering and Building Technology, Department of Construction Policy Research, Research Center for Korean Peninsula Infrastructure, Goyang 10223, Republic of Korea

The main pathways for the diffusion of chloride ions, which cause the damage in concrete structures by chloride ingress, are generally categorized into two groups: internal chloride ions introduced by the materials used during concrete mixing and external chloride ions introduced after construction (KECRI, 2014). Internal chloride ions can be generated by the cement, mixing water, and chemical admixtures used in the construction process; notably, sea sand contains approximately 0.05% salt by weight, making it the primary cause of internal chloride ingress when used as fine aggregate (Ganesan et al., 2022). The main sources of external chloride ions in structures built in marine environments include sea water. Especially in tidal zones, wet and dry cycles cause a concentration gradient on the surface, facilitating the rapid diffusion of chloride ions into the interior (Lee et al., 2023; Yoon et al., 2022). In South Korea, deicing agents are being increasingly used during the winter; calcium chloride ($CaCl_2$) and sodium chloride (NaCl) contained in the deicers can diffuse into concrete structures. Their interaction with the freeze–thaw cycles, a representative winter degradation phenomenon, can cause faster diffusion of chloride ions (Kessler et al., 2017; Zhang et al., 2017). In addition, chloride ions contained in roadside deicing agents can be transported to various concrete structures via vehicles, causing chloride ingress.

RC structures are inherently subjected to cracks over their service life owing to their high self-weight and exposure to a variety of stress conditions, given their material characteristics (Jung et al., 2018a; Ren et al., 2015; Tran et al., 2018; Wang et al., 2018). Moreover, the construction sequences of large-scale RC structures involve joints, which have vulnerabilities related to structure and durability (JSCE, 2000). Structures with such vulnerabilities experience rapid diffusion of deteriorating agents such as chloride ions into these areas, leading to localized reductions in durability (Hongming et al., 2014). By analyzing these vulnerabilities, it is possible to perform rational maintenance of structures by estimating the service life and analyzing the repair costs.

Consequently, appropriate repairs and reinforcements that consider the performance degradation caused by such chloride ingress phenomena can extend the service life of concrete structures, allowing for the economic management of maintenance costs by proposing rational maintenance techniques (Kirkpatrick et al., 2002). Maintenance cost analysis considering the service life is usually performed using deterministic analysis, which estimates the repair costs in a stepwise manner by considering the unit prices of the repair processes as simple, repetitive sums (Lee et al., 2020; Thomas & Bentz, 2002). Since the 1990s, researchers have studied probabilistic service life evaluation techniques that consider engineering uncertainties. By utilizing the degradation models for chloride ingress and carbonation, it is possible to derive the maintenance costs for the target period probabilistically, considering the initial service life, service life secured through repairs, and probabilistic variability of each life span. Unlike the results of deterministic analysis, which are presented in a stepwise manner, probabilistic analysis can present the results in the form of continuous curves (Jung et al., 2018b; Lee et al., 2020).

Therefore, this study obtained the deterministic and probabilistic chloride ingress repair costs for the RC structure under analysis, based on the results of a prior study that analyzed the service life under chloride ingress of ground granulated blast furnace slag (GGBFS) concrete considering cold joints and external load conditions. In addition, the comprehensive repair costs for the RC girder under analysis were evaluated by comprehensively considering the locations with cold joints and sections under compressive and tensile stress.

## 2 Analysis of Service Life under Chloride Ingress of Concrete Considering Cold Joints and External Force Conditions

### 2.1 Analysis Method for Chloride Diffusion Behavior Considering Cold Joints and Tensile Load Conditions

To evaluate the service life under chloride ingress by considering the vulnerabilities and load conditions, this study cited the results from prior research that evaluated the chloride diffusion coefficient of GGBFS concrete at 91 and 365 days, taking into account the cold joints and stress conditions (Oh & Kwon, 2017; Yoo & Kwon, 2016). The characteristics of the concrete mix used in the previous research are shown in Table 1.

In the previous studies (Oh & Kwon, 2017; Yoo & Kwon, 2016), cylinder specimens with a diameter of

**Table 1** Mix proportions for analysis of chloride diffusion behavior considering stress conditions and cold joint (Oh & Kwon, 2017; Yoo & Kwon, 2016)

| $G_{max}$ (mm) | Slump (mm) | S/a (%) | W/B | Air (%) | Unit weight: kg/m$^3$ | | | | |
|---|---|---|---|---|---|---|---|---|---|
| | | | | | W | Binder | | S | G |
| | | | | | | C | GGBFS | | |
| 25 | 180 | 41.4 | 0.6 | 4.5 | 180 | 180 | 120 | 735 | 1020 |

100 mm and height of 200 mm were fabricated and cut into 50 mm thickness for tensile load application, and rectangular specimens of 100×100×50 mm were prepared for compression load application. In addition, to induce cold joints, concrete was first cast into half of the mold, followed by a drying period of 24 h before casting the remaining half to create a cold joint. After evaluating the maximum compressive and tensile stresses for each aging day, accelerated chloride diffusion tests were conducted while applying compressive and tensile stresses at 30% and 60% of the maximum values, respectively. The accelerated chloride diffusion coefficient was evaluated according to Tang's method, which can be used to assess the non-steady-state chloride diffusion coefficient. In Tang's method, the accelerated chloride diffusion coefficient is evaluated by applying a 0.3 M NaOH solution to the anode and a 0.5 M NaCl solution to the cathode of the concrete specimens, followed by applying a voltage of 30 V for 8 h. After applying voltage, the specimen was split, and a silver nitrate solution (0.1 N, $AgNO_3$) was sprayed on the split side. The color-changing depth was considered as the penetration depth of chloride ions. Using the measured penetration depth, the accelerated chloride diffusion coefficient for each condition was calculated as shown in Eq. (1). The details on specimen fabrication, curing, and load application can be found in the prior study, and the process for evaluating the accelerated chloride diffusion coefficient for GGBFS concrete, considering load and cold joints, is shown in Fig. 1 (Oh & Kwon, 2017; Yoo & Kwon, 2016):

$$D_{\mathrm{rcpt}} = \frac{\mathrm{RTL}}{\mathrm{zFU}}\frac{x_d - \alpha\sqrt{x_d}}{t}, \alpha = 2\sqrt{\frac{\mathrm{RTL}}{\mathrm{zFU}}}\mathrm{erf}^{-1}\left(1 - \frac{C_d}{C_0}\right) \tag{1}$$

where $D_{\mathrm{rcpt}}$ is accelerated chloride diffusion coefficient in non-steady state condition ($m^2/s$), R is universal gas constant (8.314 J/mol K), T is absolute temperature (K), L is thickness of specimen (m), z is ionic valence (1.0), F is Faraday constant (96,500 J/V mol), U is applied potential (V), $x_d$ is penetration depth of chloride ions, $t$ is test duration time (s), $C_d$ is the chloride concentration at which the color changes when using a colorimetric method for measuring $x_d$, $C_0$ is chloride concentration in the cathode solution (mol/l), $\mathrm{erf}^{-1}$ is the inverse of the error function.

### 2.2 Analysis Results of Chloride Diffusion Behavior Considering Cold Joints and Tensile Load Conditions

Fig. 2 shows the results of the accelerated chloride diffusion tests for GGBFS concrete considering the load conditions and cold joints as per the process shown in Fig. 1 (Kwon & Oh, 2017; Yang et al., 2018; Yoo & Kwon, 2016). The diffusion coefficient of sound concrete decreased slightly under a stress load of 30% of the compressive failure stress but significantly increased under a 60% stress load. This is believed to be because the initial compression stress load reduced the chloride ion diffusivity in the concrete owing to pore consolidation, a trend that was also observed in accelerated carbonation tests in previous research (Koh et al., 2019). Under tensile stress loads, the diffusion coefficient increased linearly with the magnitude of stress, which was attributed to the vulnerability of concrete to tensile forces.

For concrete with cold joints, the behavior under tensile stress loads was similar to that of sound concrete, but under compressive stress loads, the diffusion coefficient significantly increased starting from a stress of 30% of the failure stress. This indicates that cold joint surfaces, being structurally weaker, are more strongly influenced by cracks caused by the applied compressive stress than by the effect of pore consolidation.

For analyzing the chloride diffusivity in RC girders considering load conditions, the variation in the behavior of diffusion coefficients owing to the stress conditions was quantified through regression analysis by separating the compressive and tensile areas, as shown in Fig. 3. According to Fig. 2, the diffusion coefficient of undamaged concrete decreases up to 30% of the compressive stress load, increasing the robustness against chloride ingress. However, in conservative durability performance analysis, it is considered that the diffusion coefficient does not decrease but remains constant in this range. All four cases of regression analysis showed a high determination coefficient exceeding 0.9.

### 2.3 Analysis of Service Life under Chloride Ingress for RC Girders Considering External Forces and Cold Joints

- Structural Analysis of RC Girders for Service Life Analysis under Chloride Ingress

This study performed a structural analysis assuming a two-span RC continuous girder. The results of the structural analysis and quantification of chloride ion diffusion behavior depicted in Fig. 3 were comprehensively considered to analyze the variation in the diffusion behavior according to the external forces on the RC structure. The RC girders targeted for service life analysis under chloride ingress had a length of 16 m with each span being 8 m, and the cross-sectional shape was rectangular (500 × 700 mm). The design specifics of the two-span continuous girder used in this study are shown in Table 2, and the shapes of the structure and cross section are presented in Fig. 4. The design specifics of the cross section differentiated the

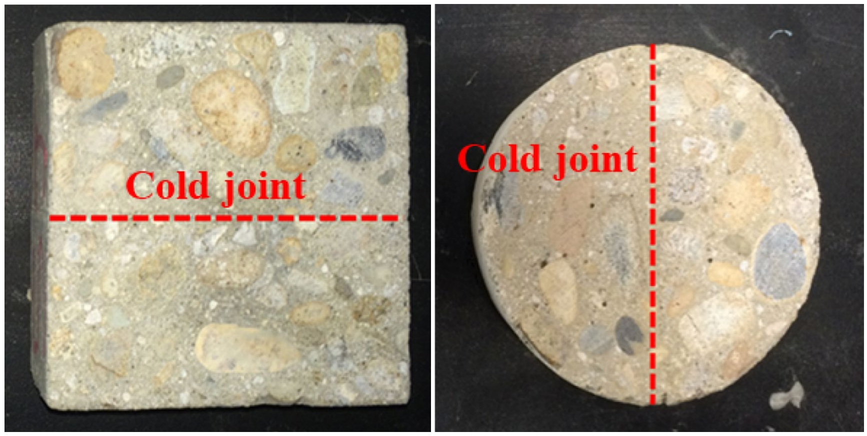


(a) Specimen with and without cold joint

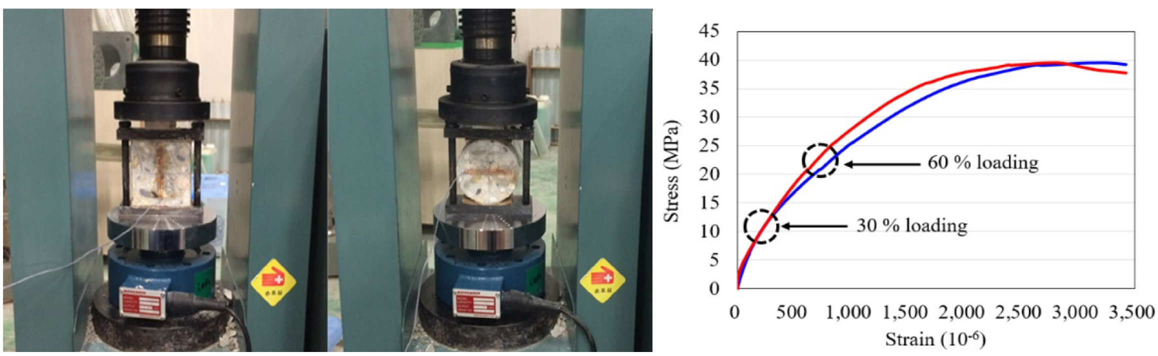


(b) Application of compressive and tensile stress considering cold joint

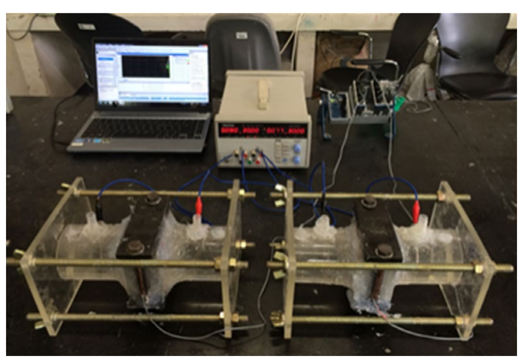

(c) RCPT considering cold joint and stress conditions

**Fig. 1** Procedure for rapid chloride permeability test (RCPT) considering cold joint and stress conditions

areas subjected to positive and negative moments, and a crack load level of 15.7 kN/m (D.L: 8.2 kN/m, L.L: 7.5 kN/m) was considered. Based on the prior research, nonlinear structural analysis according to the section lamina method was conducted to evaluate the stress behavior at each cross section of the structure at 0.5 m intervals (Yang & Kang, 2011; Yang et al., 2014). The methods and flowcharts for analyzing the compressive

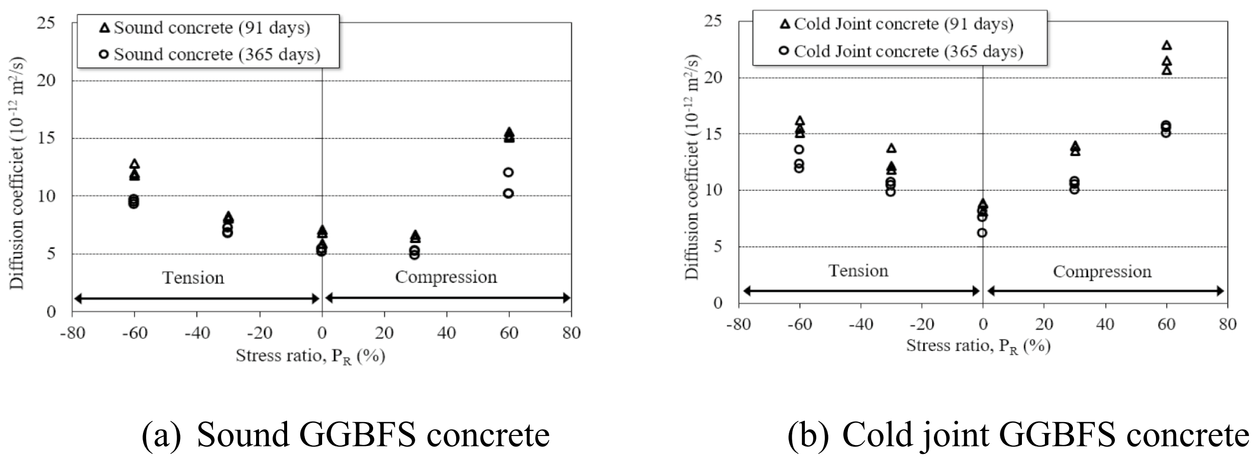


**Fig. 2** Results of accelerated chloride diffusion coefficient considering cold joint and stress conditions

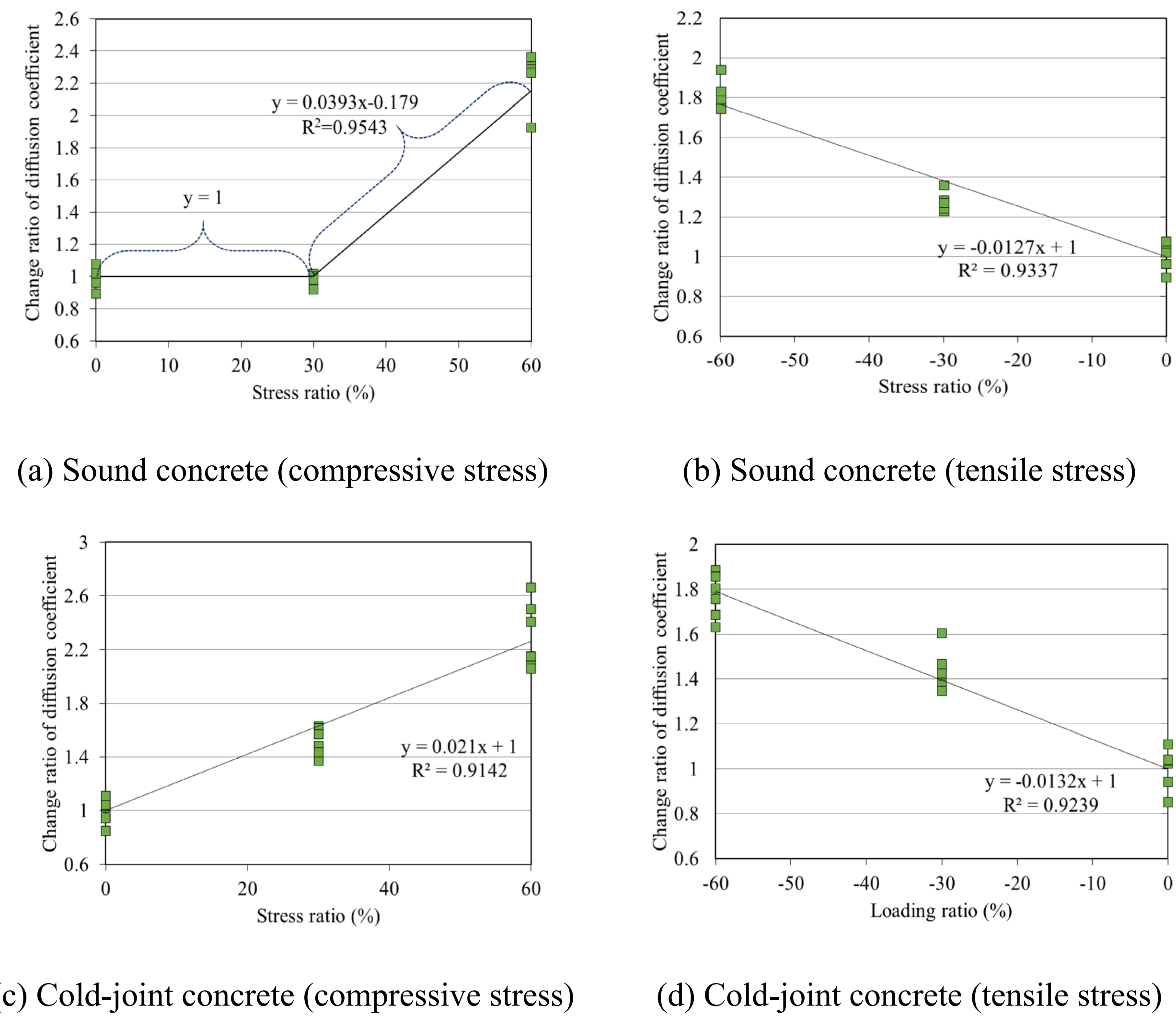


**Fig. 3** Quantification of changes in accelerated chloride diffusion coefficient considering cold joint and stress conditions

**Table 2** Design parameters of two-span continuous RC girder

| **Items** | $f_c{\prime}$ | $f_y$ | $(A_s{\prime})_{sag.}$ | $(A_s)_{sag.}$ | $(A_s{\prime})_{hog.}$ |
|---|---|---|---|---|---|
| Value | 24 MPa | 400 MPa | 567.9 mm$^2$ | 1,135.8 mm$^2$ | 1,135.8 mm$^2$ |
| **Items** | $(A_s)_{hog.}$ | $d\prime$ | d | $E_c$ | $\rho_{min}$ |
| Value | 1703.6 mm$^2$ | 51 mm | 649 mm | 25,811 MPa | 0.0035 |

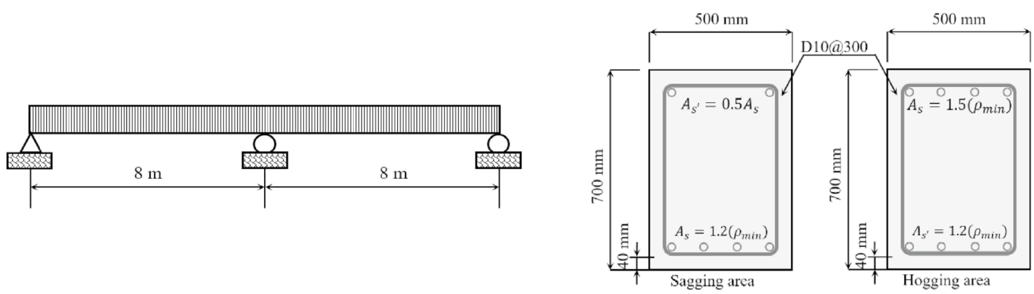


(a) The shape of RC girder (b) The section geometry

**Fig. 4** Shape and section geometry of two-span RC girder

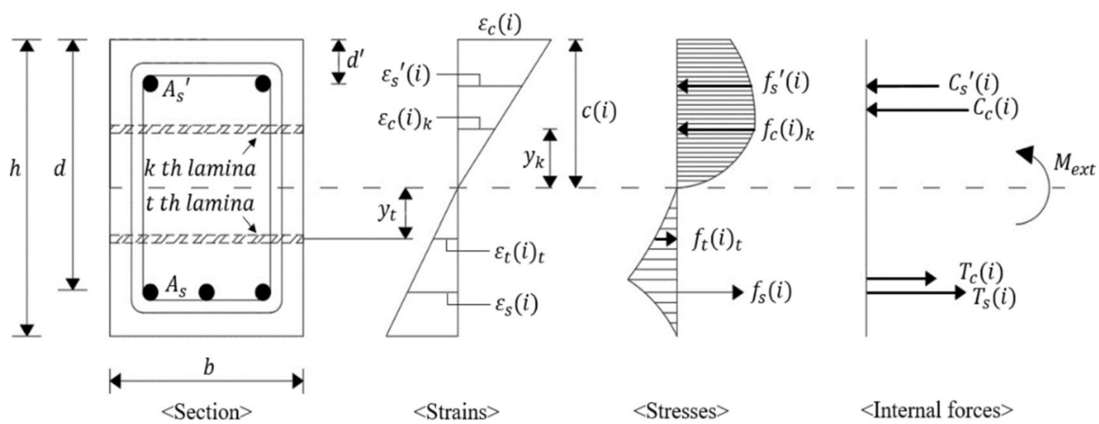


**Fig. 5** Generalized distribution of strains and stresses along the girder section under the application of a given external moment (Yang et al., 2014)

and tensile stresses at each cross section of the two-span continuous girder are shown in Figs. 5 and 6, respectively, and the results of the structural analysis are presented in Fig. 7.

- Analysis Method of Service Life Considering External Force and Cold Joint Conditions

In general, the service life of RC structures under chloride ingress is defined as the period until the chloride ion concentration at the cover depth reaches the critical chloride ion content, i.e., the concentration at which corrosion begins (ACI 365.1R, 2017; JSCE, 2007). The governing equation used in the service life analysis, that is, Fick's 2nd law, is presented in Eq. (2) (KCI, 2021):

$$C_d - C_i = (C_S - C_i) \times \left(1 - \mathrm{erf}\left(\frac{x}{2\sqrt{D_d t}}\right)\right), \qquad (2)$$

where $C_d$ represents the chloride ion content (kg/m$^3$) at location $x$ (m) and time $t$ (s), $C_i$ is the initial chloride ion content (kg/m$^3$), $C_S$ is the surface chloride ion content (kg/m$^3$), *erf* is the error function, and $D_d$ is the effective apparent chloride ion diffusion coefficient (m$^2$/s).

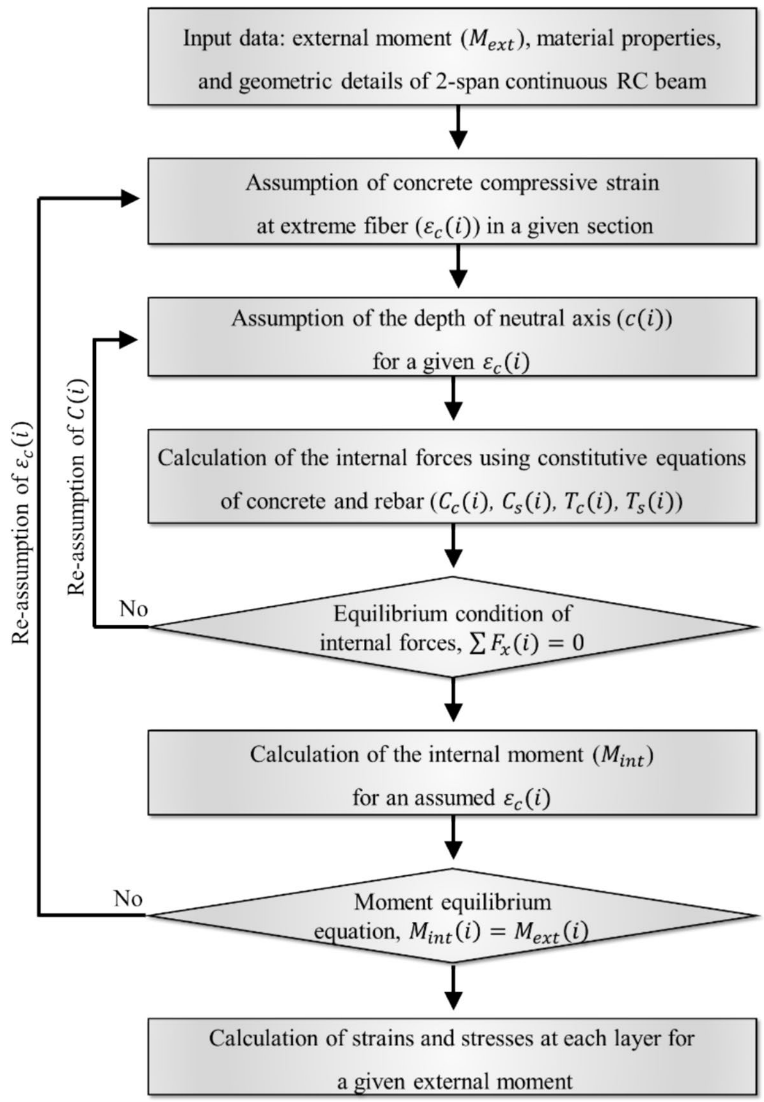


**Fig. 6** Nonlinear analytical approach for determining stresses and strains of girder section (Yang & Kang, 2011)

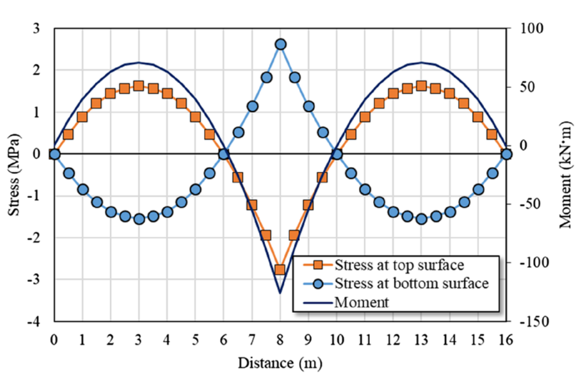


**Fig. 7** Results of nonlinear structural analysis of two-span RC girder

In Eq. (2), the effective apparent chloride ion diffusion coefficient is determined based on a division with a 30-year limit for the decrease in the diffusion coefficient, as shown in Eqs. (3) and (4). In this study, the chloride ion diffusion coefficient at the reference time was considered to increase with changes in compressive and tensile stress at different sections of the structure, based on an integrated consideration of the regression analysis results accounting for stress conditions and cold joints (as shown in Fig. 3) and the structural analysis results for a two-span RC continuous girder (Fig. 7):

$$D_d = \left(\frac{t_R}{t}\right)^m (t < 30\text{years}), \tag{3}$$

$$D_d = \frac{D_R}{1-m}\left[(1-m) + m\frac{t_c}{t}\right]\left(\frac{t_R}{t}\right)^m (t \geq 30\text{years}), \tag{4}$$

where $D_d$ represents the chloride ion diffusion coefficient ($m^2/s$) at the reference time, $t_R$ is the reference time (28 days), $t_c$ is the limit of the decrease in the diffusion coefficient (30 years), and $m$ represents the time-dependency index of the diffusion coefficient.

In Eqs. (3) and (4), the time-dependent parameter ($m$) indicates the extent to which the chloride ion diffusion coefficient decreases with the aging of the material and is generally known to be predominantly influenced by the type of binder and change in the water–binder ratio (Thomas & Bamforth, 1999; Yoon et al., 2022). Because the chloride ion diffusion coefficient in concrete continuously decreases over the maintenance period of the structure, considering the time-dependent parameter is essential for an economical and rational service life design. In this study, the time-dependent parameter model from Life-365 was used to back-calculate the diffusion coefficient at 28 days for service life analysis, as shown in Eq. (5) (Thomas & Bentz, 2002):

$$D(t) = D_R\left(\frac{t_R}{t}\right)^m, \tag{5}$$

where $D_R$ represents the apparent chloride ion diffusion coefficient ($m^2/s$) at the reference time ($t_R$), $D(t)$ is the apparent chloride ion diffusion coefficient ($m^2/s$) at time ($t$), and $t_R$ represents the reference time (28 days).

Moreover, Life-365 proposes a formula for calculating the time-dependent parameter based on the type and substitution rate of the binder, as shown in Eq. (6). This formula limits the fly ash substitution rate to a maximum of 50% and blast furnace slag powder substitution rate to a maximum of 70% (Thomas & Bentz, 2002). The flowchart for the analysis of the service life under chloride ingress according to the corresponding process is presented in Fig. 8:

$$\mathrm{m} = 0.2 + 0.4\left(\frac{\mathrm{FA}}{50} + \frac{\mathrm{SG}}{70}\right) \leq 0.6, \tag{6}$$

where FA represents the fly ash substitution rate (%) and SG represents the blast furnace slag powder substitution rate (%).

- Variables for Service Life Analysis under Chloride Ingress

The durability design standards of South Korea (KCI, 2021) suggest calculating the chloride ion diffusion coefficient based on the experimental or measured data without specifying the method of testing, such as accelerated chloride ion diffusion tests or long-term immersion tests. In addition, the chloride ingress design specifications in Japan (JSCE, 2007) propose that when using the diffusion coefficient derived from electrical acceleration tests for durability performance analysis, the accelerated chloride ion diffusion coefficient should be converted to the apparent chloride ion diffusion coefficient before use. In this study, accelerated chloride ion diffusion coefficients at 91 and 365 days were obtained through previous research, and it was found that using the accelerated chloride ion diffusion coefficient from electrical acceleration tests in service life analysis generally results in a lower evaluated service life than that observed using diffusion coefficients considering the typical outdoor marine environment. Therefore, it was deemed unsuitable to use the

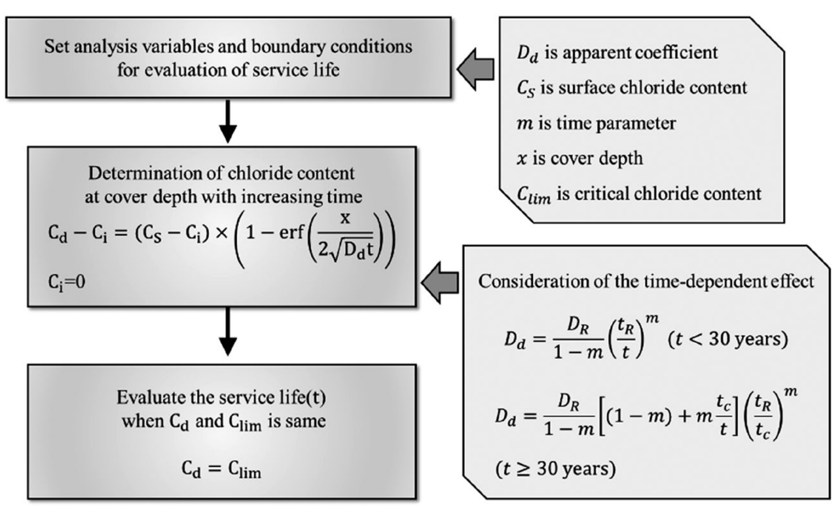


**Fig. 8** Flowchart for analysis of the service life under chloride ingress

**Table 3** Analysis variables for service life under chloride ingress

| Cover depth (mm) | Surface chloride content (kg/m$^3$) | Built up period* (year) | Critical chloride content (kg/m$^3$) | Time dependent parameter (*m*) | Annual temperature (℃) | $D_R$(x 10 m$^{-12}$/s) |
|---|---|---|---|---|---|---|
| 40 | 2.5 | 10 | 1.2 | 0.428 | 3.0–27.0 | 9.15 (Sound) 12.0 (CJ) |

* The period required for the surface chloride content to reach from "0" to the set value

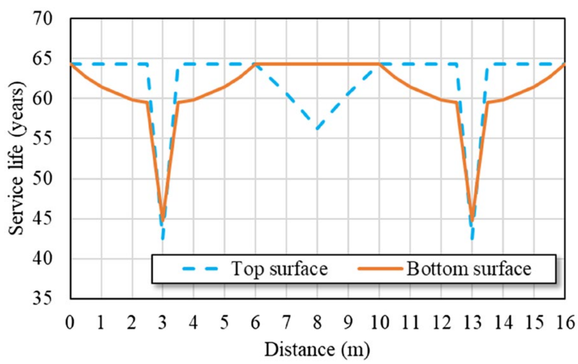


**Fig. 9** Analysis results for service life in two-span continuous RC girder considering cold joint and stress conditions

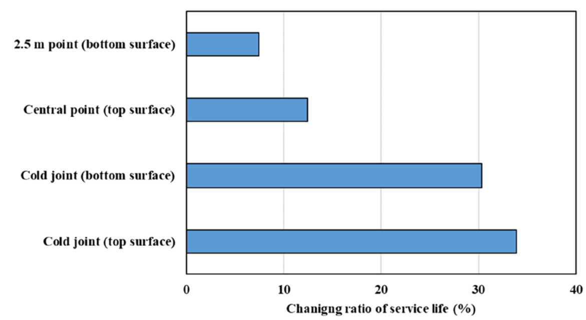


**Fig. 10** Change ratio of service life at the region with cold joint and under max tensile stress

experimental results directly for durability performance analysis, and the accelerated chloride ion diffusion coefficient was converted to the apparent chloride ion diffusion coefficient using the existing theoretical formula (Eq. 7) (Polder et al., 2007). In addition, the diffusion coefficient at 28 days was back-calculated according to Eq. (5) for use in the service life analysis. Table 3 presents the variables for analyzing the service life under chloride ingress by assuming that the target structure is located on the east coast of South Korea and setting the surface chloride content and annual temperature for 2023 (KCI, 2012):

$$D_{492} = 1.16D_{443} + 0.32 \times 10^{-12}\left(R^2 = 0.96\right), \quad (7)$$

where $D_{492}$ represents the accelerated chloride ion diffusion coefficient (m$^2$/s) according to NT BUILD 492, and $D_{443}$ indicates the apparent chloride ion diffusion coefficient (m$^2$/s) according to NT BUILD 443.

- Service Life Analysis Results for a Two-Span Continuous RC Girder Considering Load and Cold Joint Conditions

The service life of a two-span continuous RC girder, evaluated at 0.5 m intervals considering load and cold joint conditions, is presented in Fig. 9, and the assessment results on the decrease in service life at the cold joint locations and at points of maximum tensile load, based on the service life at the unaffected end points, are shown in Fig. 10.

The analysis results for service life under chloride ingress show a significant decrease in service life at the locations with cold joints in the RC girder. This is because the baseline diffusion coefficient of cold-joint concrete is higher than that of sound concrete. Furthermore, according to the regression formula in Fig. 3, the increase in diffusion coefficient is greater owing to stress. The service life at the points with cold joints, from the ends up to 3 m, showed a decrease rate of 33.9% in the upper surface and 30.3% in the lower surface when compared with the service life at the ends, where the stress conditions do not apply. Areas under tensile stress showed a slight decrease in service life, whereas those under compressive stress showed no change in service life. This was attributed to the regression formula for chloride ion diffusion behavior analyzed in this study; for the compressive stress area, it was considered that there was no change in diffusivity up to a stress level of 30% of the failure stress, and for tensile stress, the increase in diffusivity was considered linearly proportional to the magnitude of the tensile stress. After excluding the points with cold joints, the decrease in service life owing to tensile stress in the structure was 12.4% in the upper surface and 7.5% in the lower surface, with the difference in the decrease rate of service life between the upper and lower surfaces attributed to the structural analysis results. Based on the diffusion theory, it is believed that the resistance of concrete structures with discontinuities, such as cold joints, which indicate structural vulnerabilities, to issues such as chloride ingress is significantly compromised.

## 3 Probabilistic Repair Cost Analysis

### 3.1 Probabilistic Chloride Ingress Repair Cost Analysis

Based on the service life of each location of the two-span continuous RC girder evaluated in Sect. 2, this section presents the derivation of the deterministic and probabilistic maintenance costs for chloride ingress. If the service life at each location of the two-span continuous girder evaluated in Sect. 2 is referred to as $T_1$ (the first service life to occur), the period not requiring repairs is considered to have a repair frequency of "0," and the initial condition for such cases is represented in Eq. (8) (Total Information Service Corporation, 2010; Yang et al., 2020):

$$T_1 \geq T_{\text{end}}, \tag{8}$$

where $T_1$ represents the initial service life, and $T_{end}$ represents the target service life of the two-span continuous RC girder.

The standardized variable (β) and the probability of not needing repairs ($P_1$) are expressed in Eqs. (9) and (10) (Jung et al., 2018b; Yang et al., 2020), where $\overline{T_1}$ denotes the average value of the time of first repair:

$$\beta = \frac{(T_{\text{end}} - \overline{T_1})}{\sigma_1}, \tag{9}$$

$$P_1 = \int_{\beta_1}^{\infty} \frac{1}{\sqrt{2\pi}} \exp\left(-\frac{\beta^2}{2}\right) d\beta, \tag{10}$$

where $\sigma_1$ signifies the standard deviation of $\overline{T_1}$ at the time of first repair.

In addition, the condition for the number of repairs to be N occurs when $T_N$ is less than the target service life ($T_{\text{end}}$), and the sum of N and $T_{N+1}$ at the $T_N$ th repair exceeds the target service life ($T_{end}$). In this case, the probability ($P^*_{N+1}$) that the sum of the standardized variable and time of repair $T_{N+1}$ and $T_N$ exceeds the target service life ($T_{\text{end}}$) is represented in Eqs. (11) and (12) (Jung et al., 2018a, 2018b; Yang et al., 2020):

$$\beta_N = \frac{(T_{\text{end}} - (\bar{T}_N + (\bar{T}_{N+1})}{\sqrt{{\sigma_N}^2 + {\sigma_{N+1}}^2}}, \tag{11}$$

$$\begin{aligned} P^*_{N+1} &= 1 - \int_{-\infty}^{\beta_N+1} f(\beta) d\beta \\ &= \int_{\beta_N+1}^{\infty} f(\beta) d\beta \\ &= \int_{\beta_{N+1}}^{\infty} \frac{1}{\sqrt{2\pi}} \exp\left(-\frac{\beta^2}{2}\right) d\beta, \end{aligned} \tag{12}$$

where $\sigma_N$ signifies the standard deviation of $T_N$, and the failure probability when the number of repairs is N can be generalized as in Eq. (13). Furthermore, when the repair cost for a unit component (i) is fixed at $C_i$, the total repair cost is as shown in Eq. (14). Fig. 11 illustrates the concept of setting the probabilistic repair frequencies (Jung et al., 2018a, 2018b; Yang et al., 2020):

$$P_N = \left(1 - \sum\nolimits_{k=1}^{N-1} P_N\right) \times P^*_N, \tag{13}$$

$$C_T = \sum\nolimits_{k=1}^{N} (k \times C_i \times P_k), \tag{14}$$

where $C_T$ represents the sum of the total repair costs considering the repair cost of a unit component ($C_i$).

### 3.2 Analysis Variables for Probabilistic Repair Cost Analysis

To obtain the maintenance costs for chloride ingress up to the target service life of a two-span RC continuous girder, it was assumed that the initial and post-repair service lives at the cold joint area (top and bottom surface), area under maximum tensile load (8.0 m, top surface), and area not affected by the cold joint and load conditions (0.0 m) follow a normal distribution. The location where maximum tensile stress occurs at the bottom surface was not considered, as it overlapped with the cold joint area. For the analysis of repair costs, four locations, including the control case (a point unaffected by cold joint and load conditions), were selected, because significant reductions in service life were observed in remaining locations excluding the control case. In addition, to quantitatively analyze the effects of cold joints and load conditions on the repair costs, it was assumed that the same concrete mixture as used in the initial construction would be applied to the repair materials. Considering the difficulty in quality control at the cold joint area, the variability in initial service life was assumed to be 15%, whereas the variability after repair for members was assumed to be 10%. A variability coefficient of 10–20% is known to be an appropriate level for designing the durability performance of concrete structures (Kwon et al., 2009; CEB, 2006; EN 1991, 2000). The initial service life ($T_i$) and post-repair service life ($T_n$) and variability coefficients for different locations of a two-span RC continuous girder

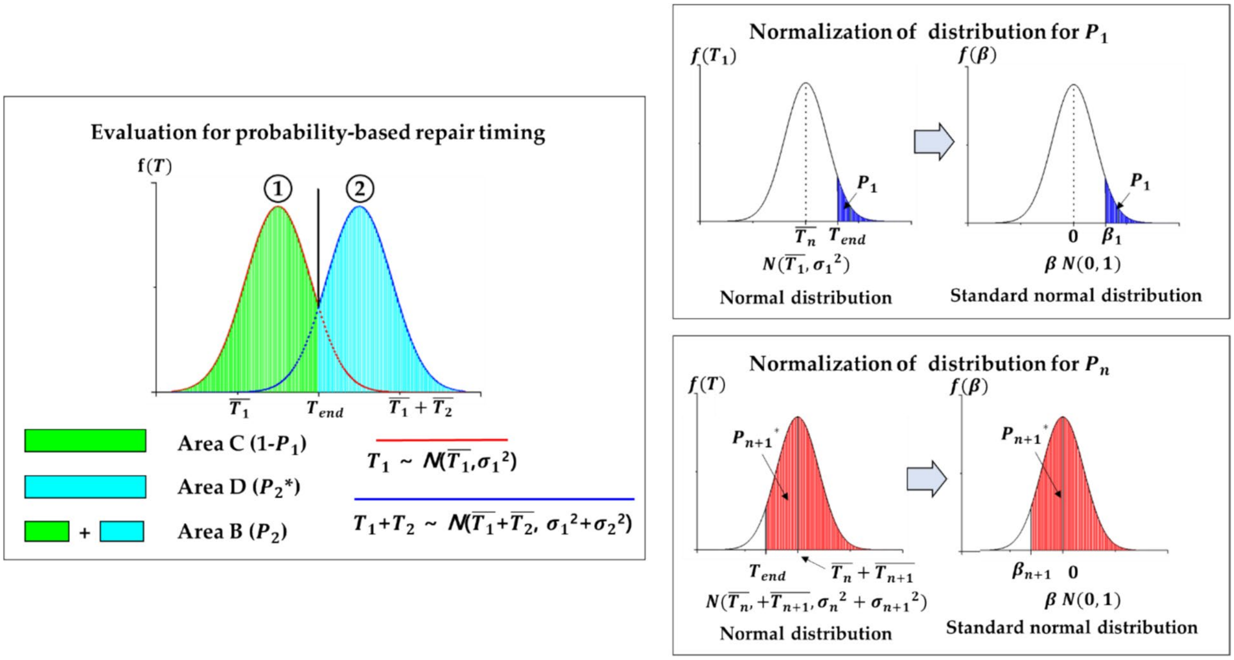


**Fig. 11** Concept of analysis of maintenance cost by probabilistic method

**Table 4** Service lives of two-span continuous RC girder before and after repair

| Location | $T_i$ (COV) | $T_n$ (COV) | Repair cost ($/m$^2$) | Target service life (years) |
|---|---|---|---|---|
| Cold joint (top surface) | 42.5 (0.15) | 64.3 (0.1) | 198.4 | 200 |
| Cold joint (bottom surface) | 44.8 (0.15) | 59.2 (0.1) | | |
| Central point (top surface) | 56.3 (0.1) | 56.3 (0.1) | | |
| Sound area | 64.3 (0.1) | 64.3 (0.1) | | |

are summarized in Table 4. By excluding the influence of the cold joint, it was considered that from the first repair onward ($T_1$), only the load affects the service life of the cold joint area. This was because the effect of cold joint was eliminated after the repair. The per-unit-area repair cost for concrete chloride ingress was based on the 2023 data provided by KPI (Korea Price Information).

### 3.3 Results of Chloride Ingress Repair Cost Analysis

- Repair Cost Estimation Results for Main Locations of a Two-Span Continuous RC Girder

The maintenance cost analysis results for chloride ingress up to the service life (200 years) for the cold joint location, point of maximum tensile load application, and sound area of the two-span continuous RC girder, considering the probabilistic variables of the initial and post-repair service lives from Table 4, are shown in Fig. 11. In deterministic repair cost analysis, it was considered that the cost increases stepwise each time the initial and post-repair service lives are reached. As shown in Fig. 12, unlike deterministic analysis methods, using probabilistic analysis techniques to estimate the repair frequency and costs allows deriving the repair frequency and costs in the form of continuous functions. This has the advantage of being able to reduce the repair frequency and costs by adjusting the target service life (Yoon et al., 2021).

In all four cases, deterministic analysis required three repairs to achieve the target service life of 200 years, whereas probabilistic analysis predicted a repair frequency of 2.74 in the sound area (*d*), and 3.0 to 3.03 in the other three cases. Similar levels of expected repair frequencies and probabilistic repair costs were estimated in cases other than the sound area, which is attributed to the sum of initial service life ($T_i$) and post-repair service life ($T_n$) relative to the set target service life. Although the deterministic analysis shows the same number of repairs and repair costs in all cases, the sound area can secure an extended service life with the same costs shortly after

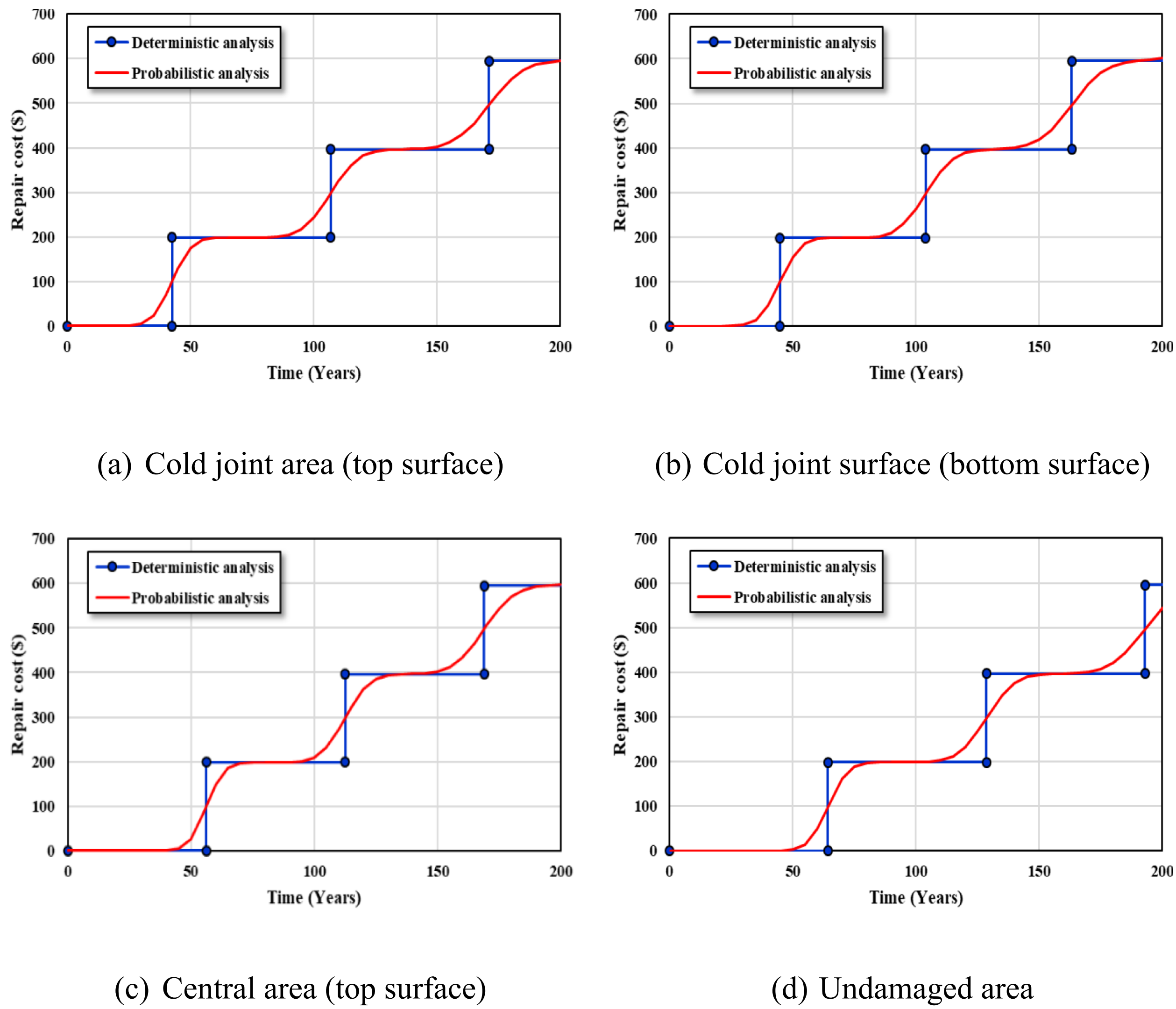


**Fig. 12** Repair cost through deterministic and probabilistic analyses

the third repair, given the target service life of 200 years. A summary of the probabilistic repair costs for achieving the target service life of 200 years in all four cases, obtained from Fig. 12, is shown in Fig. 13. In comparison with the data for the sound area, the increase rate of probabilistic repair costs at the points of tensile stress and cold joints was evaluated to be between 109.5 and 110.8%.

- Overall Repair Cost Estimation Results

This section presents an analysis of the maintenance costs associated with the extended service life of a two-span RC continuous girder. In probabilistic analysis, as costs over time are presented in the form of continuous

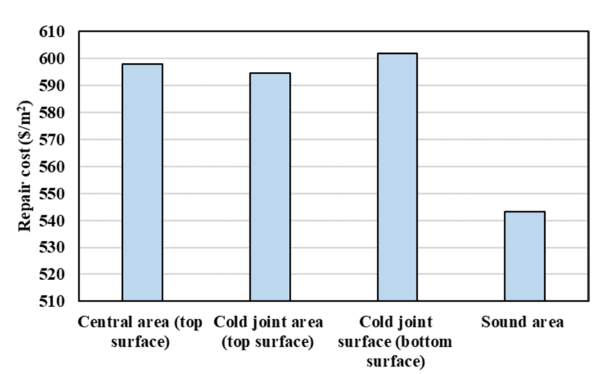


**Fig. 13** Comparison of repair costs through probabilistic analysis

functions, it is possible to calculate the repair costs for each location of the RC girder as a simple sum, whereas in deterministic methods, the total repair cost at each location must be meticulously considered. Fig. 14 presents a flowchart for deriving the total repair costs for four locations of the two-span RC girder based on the deterministic analysis results; the integrated deterministic and probabilistic repair cost behaviors for the analyzed four points are presented in Fig. 15. Here, $F_i(t)$ represents the repair costs over the service period for each location, $C_i$ represents the repair costs per location, $T_i$ represents the service life secured before/after repair for each location, and $m$ indicates the repair frequency.

In Fig. 15, there is very little difference in the final repair cost between deterministic and probabilistic analysis methods, with probabilistic repair costs being higher in some intervals. This is because of the negative effect of the coefficient of variation (COV), whereas in intervals where the COV has a positive effect, probabilistic repair costs are lower than the deterministic costs. Furthermore, during probabilistic analysis, the higher the COV, the greater is the extent to which the results tend to smooth into a continuous function curve, with economically feasible repair opportunities existing between 40 and 50% of the respective service life following deterministic repair times. The final repair costs were analyzed to be 2777.6 $/m$^2$ in deterministic analysis and 2337.6 $/m$^2$ in probabilistic analysis. Moreover, the yellow circled areas indicate a significant increase in repair cost over a short period, which is attributed to the reduced service life at the cold joint and points of application of the maximum tensile load. Therefore, cold joints and stress conditions have a significant effect on the increase in repair costs of RC structures. Extending the service life at the cold joint and points

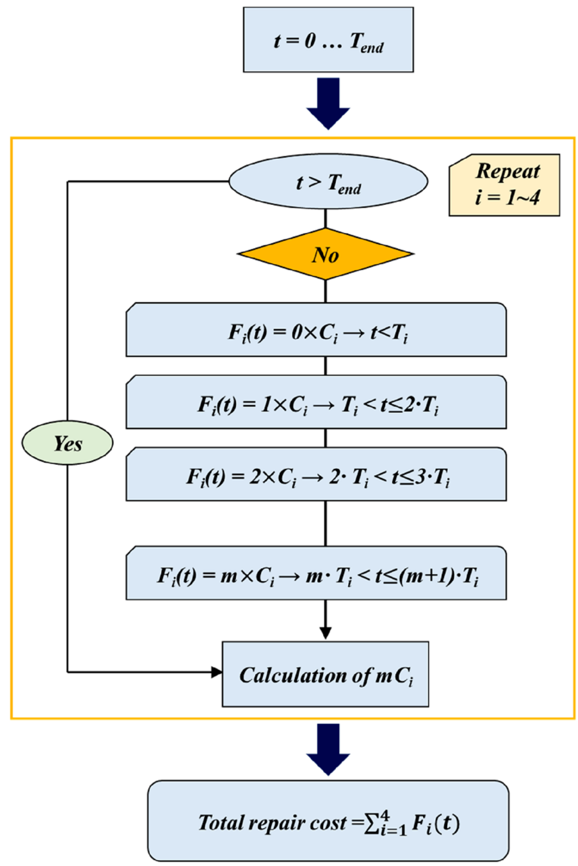


**Fig. 14** Calculation flowchart for total repair cost in deterministic method

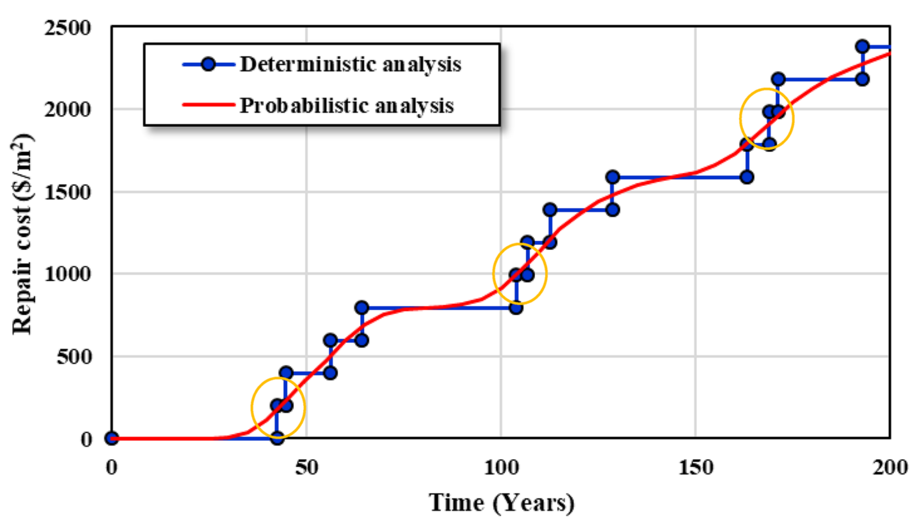


**Fig. 15** Total repair cost considering multiple points of two-span continuous RC girder using deterministic and probabilistic analyses

of application of tensile stress as much as possible and setting a target service life considering this strategy could enable economical maintenance against chloride ingress in RC structures. In addition, this study considered only the repair costs for chloride ingress, assuming uniform costs. If the different repair costs for various degradation phenomena were considered, it could identify the dominant degradation factors affecting the maintenance costs up to the target service life.

## 4 Conclusion

This study derived the service life after chloride ingress and deterministic and probabilistic repair costs under cracking load conditions of a two-span RC continuous girder by applying the accelerated chloride diffusion coefficient results for GGBFS concrete considering cold joint and load conditions from previous research. In probabilistic repair cost analysis, the initial service life and post-repair service life for each location were assumed to follow a normal distribution, and the overall increase in repair cost for the RC continuous girder with increased service period was analyzed. The conclusions of this study are as follows.

1) The service life for chloride ingress at various locations considering cold joints and stress conditions was evaluated by comprehensively considering the chloride diffusion coefficient test results from previous research along with the structural analysis results of the RC continuous girder. Service life significantly decreased at locations with cold joints owing to the higher baseline diffusion coefficient of the cold-joint concrete when compared with that of sound concrete and greater increase in diffusion coefficient owing to stress. In comparison with the service life at areas unaffected by stress and cold joints, the cold joint area showed a decrease in service life of 33.9% in the upper surface and 30.3% in the lower surface. The presence of tensile stress also tended to decrease the service life, with the points of maximum tensile stress application experiencing a decrease of 12.4% in the upper surface and 7.5% in the lower surface. Based on the diffusion theory, cold joint areas, which have structural and durability vulnerabilities, appear to be susceptible to degradation phenomena such as chloride ingress.
2) This study analyzed both deterministic and probabilistic repair costs for a two-span RC continuous girder up to the target service life. Probabilistic analysis, which considers the service life as a random variable following a specific distribution, allows for rational adjustments to repair costs. As a result, unlike the stepwise cost increases observed in deterministic analysis, probabilistic analysis presented a continuous cost increase function. At a target service life of 200 years, similar repair costs were derived between the two methods when excluding undamaged areas. However, the probabilistic approach allows for more cost-effective maintenance by adjusting the target service life in response to the cost-impacting effect of COV. The sound area showed the lowest expected repair frequency of 2.74, whereas the cold joint and maximum tensile stress application areas showed an increase in the probabilistic repair costs by 109.5 to 110.8% when compared with that of the sound area.
3) The maintenance costs for a two-span RC continuous girder were analyzed by comprehensively considering the cold joint and tensile stress application areas. In intervals where the COV had a negative impact, probabilistic repair costs were evaluated to be higher than the deterministic costs, whereas in intervals with a positive effect of the COV, probabilistic repair costs were lower than the deterministic costs. The final repair costs were analyzed to be 2777.6 $\$/m^2$ in deterministic analysis and 2337.6 $\$/m^2$ in probabilistic analysis. Given the significant effects of cold joints and tensile stress conditions on the behavior of the increase in repair cost, extending the service life at these points and setting a target service life considering these factors would enable economical maintenance.

**Author contributions**

SJK conducted conception, proposed analysis method and modeling, wrote original draft. KML conducted review, investigated previous studies. KCK conducted data curation and review. KTK checked the proposed analysis method, supervised entire research, YSY processed the data, wrote original draft, revision and editing. All the authors read and approved the final manuscript.

**Funding**

Research for this paper was carried out under the KICT Research Program (Project No. 20240157-001, Development of concrete bridge repair materials and methods customized for cold weather regions using SUPER concrete) funded by the Ministry of Science and ICT.

**Availability of data and materials**

The authors agree to provide any supporting data upon reasonable request.

## Declarations

**Competing interests**

The authors declare no competing interests.

Received: 26 May 2024 Accepted: 25 December 2024
Published online: 20 March 2025

**References**
ACI 365.1R-17. (2017). *Report on service life prediction*. ACI Committee 365, American Concrete Institute.
CEB. (2006). *Model code for service life design*. The International Federation for Structural Concrete (fib), Task Group 5.6.16.
EN 1991. (2000). *Eurocode 1: Basis of design and actions on structures*. European Committee for Standardization.
Ganesan, K., Kanagarajan, V., & Dominic, J. R. J. (2022). Influence of marine sand as fine aggregate on mechanical and durability properties of cement mortar and concrete. *Materials Research Express, 9*(3), 035504. https://doi.org/10.1088/2053-1591/ac5f88
Hongming, L., Jin, W., Yongji, S., & Zhe, W. (2014). Effect of external loads on chloride diffusion coefficient of concrete with fly ash and blast furnace slag. *Journal of Materials in Civil Engineering, 26*(9), 04014053. https://doi.org/10.1061/(ASCE)MT.1943-5533.0000941
JSCE. (2000). *Cold joint problems and countermeasures in concrete structures*. Japan Society of Civil Engineers.
JSCE. (2007). *Standard specification for concrete structures—Design*. JSCE-Guidelines for Concrete 15, Japan Society of Civil Engineering.
Jung, S. H., Ryu, H. S., Karthick, S., & Kwon, S. J. (2018a). Time and crack effect on chloride diffusion for concrete with fly ash. *International Journal of Concrete Structures and Materials, 12*, 14. https://doi.org/10.1186/s40069-018-0230-2
Jung, S. H., Yang, H. M., Yang, K. H., & Kwon, S. J. (2018b). Maintenance for repaired RC column exposed to chloride attack based on probability distribution of service life. *International Journal of Concrete Structures and Materials, 12*, 22. https://doi.org/10.1186/s40069-018-0259-2
KCI. (2012). *Concrete standard specification-durability part*. Korea Concrete Institute.
KCI. (2021). *KDS 14 20 40-Durability design standard for concrete structures*. Korea Concrete Institute.
KECRI. (2014). *A study on the durability design and assessment of concrete structures by chloride attack under de-icing salt environments, research report* (Korea Expressway Corporation Research Institute, No. 2014-43-534.9607).
Kessler, S., Thiel, C., Grosse, C. U., & Gehlen, C. (2017). Effect of freeze–thaw damage on chloride ingress into concrete. *Materials and Structures, 50*, 1–13.
Kirkpatrick, T. J., Weyers, R. E., Anderson-Cook, C. M., & Sprinkel, M. M. (2002). Probabilistic model for the chloride-induced corrosion service life of bridge decks. *Cement and Concrete Research, 32*(12), 1943–1960.
Koh, T.-H., Kim, M.-K., Yang, K.-H., Yoon, Y.-S., & Kwon, S.-J. (2019). Service life evaluation of RC T-girder under carbonation considering cold joint and loading effects. *Construction and Building Materials, 226*, 106–116.
Kwon, S. J., Na, U. J., Park, S. S., & Jung, S. H. (2009). Service life prediction of concrete wharves with early-aged crack: Probabilistic approach for chloride diffusion. *Structural Safety, 31*(1), 75–83.
Lee, H. M., Lee, H.-S., Suraneni, P., Singh, J. K., & Mandal, S. (2020). Prediction of service life and evaluation of probabilistic life-cycle cost for surface-repaired carbonated concrete. *Journal of Materials in Civil Engineering, 32*(10), 4020297. https://doi.org/10.1061/(ASCE)MT.1943-5533.0003390
Lee, J.-S., Yang, K.-H., Yoon, Y.-S., Nam, J.-W., & Kwon, S.-J. (2023). Service life evaluation of HPC with increasing surface chlorides from field data in different sea conditions. *Advances in Concrete Construction, 16*(3), 155–167.
Lee, S. K., & Zielske, J. (2014). *An FHWA special study: post-tensioning tendon grout chloride thresholds* (Federal Highway Administration, FHWA-HRT-14-039).
Mehta, P. K., & Monteiro, P. M. (2009). *Concrete-structure, properties, and materials* (2nd ed., pp. 113–171). Prentice Hall.
Oh, K.-S., & Kwon, S.-J. (2017). Chloride diffusion coefficient evaluation in 1 year-cured OPC concrete under loading conditions and cold joint. *Journal of the Korea Institute for Structural Maintenance and Inspection, 21*(5), 21–29.
Polder, R. B., van der Wegen, G., & Boutz, M. (2007). Performance based guideline for service life design of concrete for civil engineering structures—A proposal discussed in the Netherlands. *International RILEM Workshop on Performance Based Evaluation and Indicators for Concrete Durability*, Madrid, Spain (pp. 31–39).
Ren, Y., Huang, Q., Liu, Q. Y., Sun, J. Z., & Liu, X. L. (2015). Chloride ion diffusion of structural concrete under the coupled effect of bending fatigue load and chloride. *Materials Research Innovations, 19*, 181–184.
Thomas, M. D. A., & Bamforth, P. B. (1999). Modelling chloride diffusion in concrete: Effect of fly ash and slag. *Cement and Concrete Research, 29*(4), 487–495.
Thomas, M. D. A., & Bentz, E. C. (2002). Computer program for predicting the service life and life-cycle costs of reinforced concrete exposed to chlorides. *Life365 Manual*, *SFA*, (pp. 12–56).
Total Information Service Corporation. (2010). *TOTAL-LCC, Technical Manual, ver.1.1* (2nd ed., pp. 24–28) Total Information Service Corporation.
Tran, T. T., Truong, Q. V., Ranaivomanana, H., & Khelidj, A. (2018). Effect of pre-loading on chloride diffusion in concrete. *Journal of Asian Concrete Federation, 4*(1), 22–28.
Wang, Q., Sun, W., Guo, L., Gu, C., & Zong, J. (2018). Prediction of chloride ingress in steel fibre reinforced concrete under bending load. *Ceramics-Silikáty, 62*, 59–66.
Yang, H.-M., Lee, H.-S., Yang, K.-H., Ismail, M. A., & Kwon, S.-J. (2018). Time and cold joint effect on chloride diffusion in concrete containing GGBFS under various loading conditions. *Construction and Building Materials, 167*, 739–748.
Yang, K.-H., & Kang, T.H.-K. (2011). Equivalent strain distribution factor for unbonded tendon stress at ultimate. *ACI Structural Journal, 108*(2), 217–226.
Yang, K.-H., Lim, H.-S., Kwon, S.-J., & Kim, J.-H. (2020). Repair cost estimation techniques for reinforced concrete structures located at the seashore: Considering various probabilistic service life functions and actual mix proportions. *Construction and Building Materials, 256*, 119469. https://doi.org/10.1016/j.conbuildmat.2020.119469
Yang, K.-H., Mun, J.-H., Cho, M.-S., & Kang, T.H.-K. (2014). Stress-strain model for various unconfined concretes in compression. *ACI Structural Journal, 111*(4), 819–826.
Yoo, S. W., & Kwon, S.-J. (2016). Effects of cold joint and loading conditions on chloride diffusion in concrete containing GGBFS. *Construction and Building Materials, 115*(2016), 247–255.
Yoon, Y.-S., Ahn, Y.-H., Wang, X.-Y., & Kwon, S.-J. (2021). Total repair cost simulation considering multiple probabilistic measures and service life. *Sustainability, 13*(4), 2350. https://doi.org/10.3390/su13042350
Yoon, Y.-S., Lee, J.-S., Min, J.-Y., & Kwon, S.-J. (2022). Behavior of apparent chloride diffusion coefficient of fly ash concrete under long-term marine exposure. *Advances in Concrete Construction, 14*(6), 369–380.
Yoon, Y.-S., Ryu, H.-S., Lim, H.-S., Koh, K.-T., Kim, J.-S., & Kwon, S.-J. (2018). Effect of grout conditions and tendon location on corrosion pattern in PS tendon in grout. *Construction and Building Materials, 186*, 1005–1015.
Zhang, P., Cong, Y., Vogel, M., Liu, Z., Müller, H. S., Zhu, Y., & Zhao, T. (2017). Steel reinforcement corrosion in concrete under combined actions: The role of freeze-thaw cycles, chloride ingress, and surface impregnation. *Construction and Building Materials, 148*, 113–121.

## Publisher's Note



**Seung-Jun Kwon** is a professor at Department of Civil and Environmental Engineering, Hannam University, Daejeon 34430, Korea.

**Kwang-Mo Lim** is a senior researcher at Research Center for Korean Peninsula Infrastructure, Department of Construction Policy Research, Korea Institute of Civil Engineering and Building Technology, Goyang 10223, Korea.

**Kyong-Chul Kim** is a senior researcher at Research Center for Korean Peninsula Infrastructure, Department of Construction Policy Research, Korea Institute of Civil Engineering and Building Technology, Goyang 10223, Korea.

**Kyung-Taek Koh** is a senior research fellow at Research Center for Korean Peninsula Infrastructure, Department of Construction Policy Research, Korea Institute of Civil Engineering and Building Technology, Goyang 10223, Korea.

**Yong-Sik Yoon** is a post-doctoral researcher at Research Center for Korean Peninsula Infrastructure, Department of Construction Policy Research, Korea Institute of Civil Engineering and Building Technology, Goyang 10223, Korea.